

Biometric Authentication Based on Auscultated Heart Sounds in Healthcare

Mizuho Tagashira and Takafumi Nakagawa, *Member, IAENG*

Abstract—Even though updating reference data is required for stable personal authentication, updating previously collected biometric data is very difficult. In this paper, we proposed a biometric authentication system based on heart sounds that is compatible with healthcare systems. Our system prevents heart disease by detecting abnormal heart sounds while collecting biometric data. The same features, which are used in personal authentication and healthcare, are computed from the temporal changes of sound power calculated from time-frequency analysis. The Mahalanobis-Taguchi method discriminates the differences between referenced and measured heart sounds. We experimentally evaluated our system's performance and achieved an authentication rate of 90-100% on ten research participants and 100% recognition rate for 19 disease cases of heart murmurs.

Index Terms—Mahalanobis-Taguchi method, heart sound, Mahalanobis distance, biometric authentication

I. INTRODUCTION

RECENT personal authentication research, based on biometric signals, has made personal authentication more secure than inputting passwords. In biometric authentication, image data or biomedical signals are used as biological information that indicate personal characteristics. Authentication with such image data as fingerprints, palm prints, blood vessel shapes, irises, or faces has already been applied in many fields [1-2]. However, such systems sometimes misidentify counterfeiters that are imitating a part of the human body [2-5]. Such biological signals as pulse waves, ECGs, or heart sounds provide greater robustness than image data because disguises are impossible. Unfortunately, much biometric data are required to create reference data. Updating them is also necessary for stable personal authentication over a long period of time. Therefore, how to collect biometric data during acquisitions remains complicated. Some works applied ECGs or pulse waves collected by healthcare services to biometric authentication [6-8]. But for heart sounds, past works separately reported biometrics research and healthcare management applications. No biometric authentication system has been proposed for healthcare applications. However, heart sound data can be efficiently accumulated by applying diagnosis based on heart sounds to health care. A healthcare system is needed to prevent such lifestyle diseases as those caused by westernized eating habits, changes in working environments, and

Mizuho Tagashira is with the Brain Attack Center, Ota Memorial Hospital, 3-6-28, Okinogamicho, Fukuyama, Hiroshima, Japan
E-mail: c/o t-nakagawa@kgw.bunri-u.ac.jp

Takafumi Nakagawa is with the Tokushima Bunri University, Health and Welfare Department, 1314-1, Shido, Sanyuki, Kagawa, Japan
E-mail: t-nakagawa@kgw.bunri-u.ac.jp

insufficient exercise. Lifestyle diseases increase heart disease, which is the world's leading cause of death [9]. Since lifestyle diseases are rarely indicated until the outbreak of a serious symptom, heart disease might progress completely unnoticed. Therefore, we must observe a person's health condition over a long period of time. If abnormal heart sounds are detected at an early stage, heart disease can be prevented. Discriminating heart disease from heart sounds is critical to select features in which a clear difference between normal and abnormal sounds appears. In many works, the power spectrum (PS), Mel Frequency Cepstral Coefficients (MFCC), wavelet coefficients, or frequency components are used as the features of heart sounds. Since these features do not refer directly to the time variation of auscultated signals which physicians easily understand, supporting re-auscultation is difficult. On the other hand, neural networks, support vector machines, nearest neighbor methods, and Gaussian mixture models have been proposed to discriminate among individuals and abnormal heart sounds [10-21]. These methods effectively judge individuals and classify heart sounds into disease cases. However, abnormal heart sounds have various degrees and types among individuals. Therefore, another problem is how to collect much abnormal data. Estimating the degree of abnormality is also difficult.

In this paper, we proposed a user-friendly biometric system that works with healthcare systems based on the collection of heart sounds. Thus, reference data must be periodically updated for biometric authentication. We used identical features in the biometric authentication and detection of abnormal heart sounds and calculated them from temporal sound power, which was obtained by summing up the PS components calculated from the time-frequency analysis of heart sounds. The difference between the reference data and the measured heart sounds is evaluated as the Mahalanobis distance (MD) by the Mahalanobis-Taguchi (MT) method. Related papers have studied the relationship between MD values and medical condition changes or the severity of hepatitis, medical conditions, and treatment effects from the magnitude of MD values [22-23]. However, to the best of our knowledge, no reports have detected abnormal heart sounds with the MT method.

II. CARDIAC DYNAMICS AND HEART SOUNDS

In this section, we first explain the relationship between cardiac dynamics and heart sounds. Fig. 1 shows the heart valves [24]. Fig. 2 shows the relationship between heart sounds and cardiac dynamics [25]. The heart's four cardiac valves (mitral, aortic, tricuspid, and pulmonary) open and

close to allow blood flow throughout the body. Heart sounds are caused by the reverberation of blood by the closing of cardiac valves or its turbulent flow into ventricles. The two predominate sounds in a normal heart are the first heart sound (S1) and the second heart sound (S2). Extra heart sounds are also present: the third heart sound (S3), the fourth heart sound (S4), the mitral valve opening sound, and a click sound. S1 represents the normal closing of the mitral and tricuspid valves. S1 is heard most clearly at the heart's apex. S2 is generated by the closure of the aortic and pulmonary valves. A cardiac cycle, which repeats the contraction and expansion and is divided into ventricular systole and ventricular diastole, is a cycle of a S1 pair. The interval between S1 and S2 is the systole; the interval between S2 and the next S1 is the diastole. Extra heart sounds are present during the diastole. When dysfunction or stenosis occurs at the aortic or mitral valves, blood turbulence occurs near the valves. Heart murmurs are generated as a result of the turbulent flow of blood. Since heart murmurs do not occur in a normal heart, they indicate cardiovascular disease.

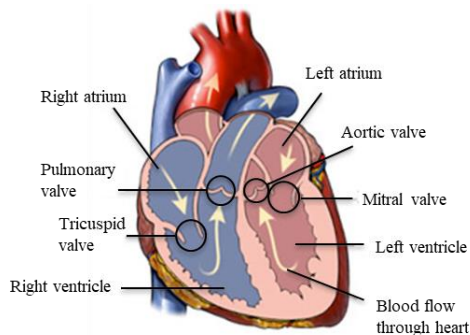


Fig. 1 Heart valve

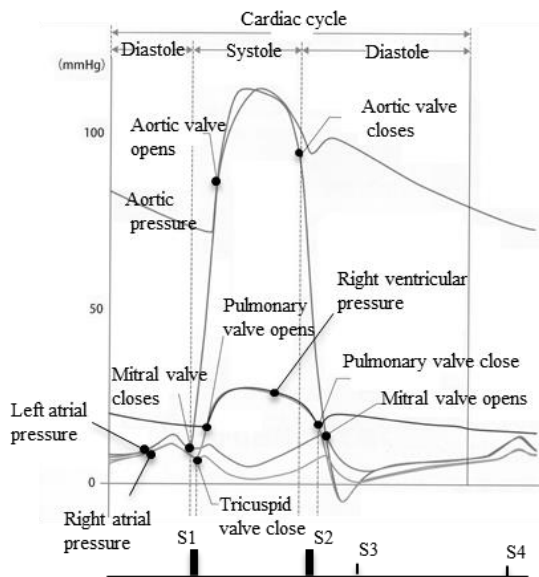


Fig. 2 Cardiac cycle and generation of heart sounds

III. HEART SOUND ANALYSIS METHOD

In this paper, we only used the heart sounds auscultated at the apex. The MT method is used for the authentication and detection of abnormal heart sounds. In the following, we first describe the selected features and their calculation procedures

and then MT's calculation procedure. Since we calculated the cardiac cycle under conditions where the amplitude of S1 exceeds that of S2, we only used the heart sounds at the heart's apex.

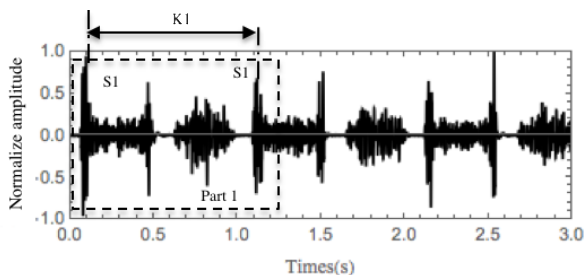
A. Selection of features

This subsection presents the features and their calculation procedures. In our system, the same kinds of features are used in biometric authentication, and the detection of abnormal heart sounds allows physicians to easily understand their changes. We calculated the following eight features: K1-K8. Six (K2-K7) detected abnormal heart sounds. Seven (K2-K8) are used for personal authentication.

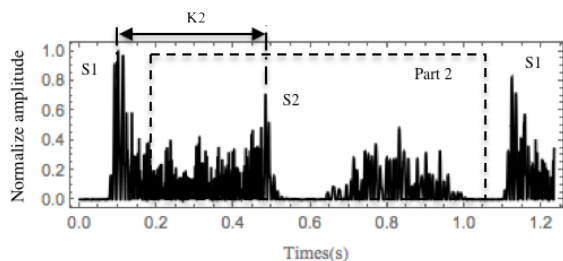
Figure 3 shows the procedure for calculating the features. Fig. 3(a) is an example of the abnormal heart sounds recorded in a training workbook's CD recorded from actual patients for a medical staff [25]. The vertical axes show the amplitudes normalized by a maximum value. The heart murmurs caused by ventricular septal defects are observed during ventricular systole and ventricular diastole. Fig. 3(b) is the modified waveform in part 1 in Fig. 3(a). A signal is made by subtracting the baseline from the original waveform. Part 2 is a 100 ms area inside the two S1 time positions. K1 is an interval of S1, and K2 is the interval between S1 and S2. The S1 and S2 positions are calculated from the peak detection of a cubic spline curve generated by 100 data points. Although some peak points are calculated, they are scrutinized by the following procedures. The normal resting heart rate is between 50 and 120 beats per minute. Considering its variations, K1 is assumed to be between 0.5 s and 1.25 s. K2 is empirically located between 125 ms and half of the interval of K1. Fig. 3(c) shows the temporal sound power $w(t)$, which is calculated by summing up all the PS components within a window function on a signal. The vertical axis is normalized by the maximum value. PS is calculated by the short-time Fourier transform whose frequency content changes over time into the time-frequency domain by shifting a window on a signal. We used a rectangular window as a window function. Since the main component of the normal heart sound frequency is about 20-200 Hz and abnormal heart sounds are observed at about 20-400 Hz [26], the window function's width is determined to be a frequency resolution of about 400 Hz. L1 to L4 show the integral width for calculating the K3-K6 features. Since the S1 and S2 duration is 40-150 ms [27], we selected time widths of L1 and L2 as ± 100 ms. Therefore, L3 and L4 are uniquely determined. L3 is from the 100 ms point after S1 to the 100 ms point before S2. L4 is from 100 ms after S2 to 100 ms before the next S1.

K3 is an integrated value of $w(t)$ over L1, and K4 is an integrated value of $w(t)$ over L2. K3 and K4 comprehensively evaluate the duration time and the amplitude fluctuation at S1 and S2. The integration over L3 is K5, and K6 is the integrated values over L4. K5 and K6 evaluate heart murmurs, which are almost zero in normal heart sounds. K7, which is the amplitude at S2, can evaluate the relative change between S1 and S2. For example, K7 decreases as the amplitude of S1 increases due to the rapid closing of the mitral valve. Although not shown in Fig. 1, K8 is an integrated value of $w(t)$ over time between two S1s. K8 is only used for biometric authentication. Since K1 changes depending on the fluctuation of the heart rate, the physical condition, and the

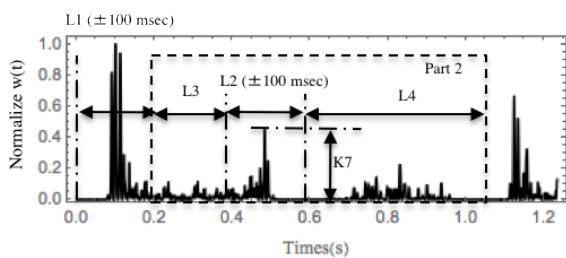
measurement environment, it is not used as a feature. The other features are normalized by the length of K1. A physician determines abnormal heart sounds based on the rhythm of the auscultation sound. First, S1 and S2 sounds are identified from the auscultation sound, and the abnormal sounds in the systole and diastole are estimated by using them. Therefore, the features used in this paper directly correspond to the temporal change of heart sounds and will be helpful to physicians at re-examinations.



(a) Example of abnormal heart sounds



(b) Modified waveform between two S1s



(c) Sound power $w(t)$

Fig. 3 Procedure to calculate features

B. Classification method

The MT method, which is used for classification, is a diagnosis approach for various multivariate data. MD is used as a measurement scale. A set of features is standardized and a unit space (normal group) is created and used as a frame of reference for the MT method’s measurement scale. We calculated the square MD value (D^2) from the inverse matrix of correlation matrix (R) by Eq. (1). [27]:

$$D_i^2 = \frac{1}{k} U_i R^{-1} U_i^T, \tag{1}$$

where i is the amount of data, k is the kind of feature, $U_i = (u_{i1}, \dots, u_{ik})$, and u_{ik} is the i -th data standardized by average value \bar{x}_j and standard deviation σ_j of k -th feature as follows:

$$u_{ik} = \frac{x_{ik} - \bar{x}_k}{\sigma_k}. \tag{2}$$

The average MD for the normal group is unity. The MT

method assumes that the feature distributions are normally distributed. The discrimination accuracy decreases when the distribution deviates from a normal distribution [28-29]. Since K5 and K6 are almost zero in normal heart sounds, the values of their features are replaced by data that are randomly created based on the average and standard deviations used in the standardized process. This data reconstruction process is repeated until the MD average calculated for the unit space is almost unity. In abnormal heart sound analysis, the main features, which increase the MD values, are decided by a two-level L_{12} mixed-type orthogonal array. The main features are selected by ANOVA under a condition where p -value $< 5\%$. MD values are recalculated using the selected features obtained from the above procedure. Table I is the calculation result of the abnormal heart sound shown in Fig. 3. In the calculation, there are six features, so columns 7 to 11 are not allocated. “1” or “2” in Table 1 indicates whether a feature was used. η is the result calculated by the combination of features shown in experiments 1 to 12. Here η is estimated by Eq. (3), where M is the average of the MD values. When the MD value increases, η ’s value grows and is closer to the group of abnormalities:

$$\eta = -10 \log_{10} \frac{1}{M}. \tag{3}$$

A factorial effect diagram created from Table I is shown in Fig. 4. The interaction among the factors is ignored. The horizontal axis is the features. For example, 1 and 2 indicate whether a feature was used to calculate MD. Fig. 4 shows that the main effect is the K5 and K6 features. This result agrees with the signal characteristics shown in Fig. 3(a). Identifying the key features helps physicians perform re-auscultation. On the other hand, for biometric authentication, we calculated the maximum MD value with a round robin of feature combinations because the key features that satisfy p -value $< 5\%$ are not found by ANOVA analysis in some cases.

Table I
 η calculated by orthogonal arrays

Exp. No	features						no allocation					Calc. η
	K2	K3	K4	K5	K6	K7	7	8	9	10	11	
1	1	1	1	1	1	1	1	1	1	1	1	36.0
2	1	1	1	1	1	2	2	2	2	2	2	36.0
3	1	1	2	2	2	1	1	1	2	2	2	14.4
4	1	2	1	2	2	1	2	2	1	1	2	13.8
5	1	2	2	1	2	2	1	2	1	2	1	36.0
6	1	2	2	2	1	2	2	1	2	1	1	29.4
7	2	1	2	2	1	1	2	2	1	2	1	29.7
8	2	1	2	1	2	2	2	1	1	1	2	35.9
9	2	1	1	2	2	2	1	2	2	1	1	5.8
10	2	2	2	1	1	1	1	2	2	1	2	36.0
11	2	2	1	2	1	2	1	1	1	2	2	29.7
12	2	2	1	1	2	1	2	1	2	2	1	35.9

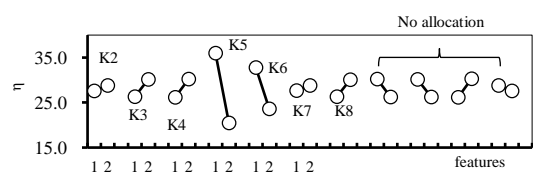


Fig. 4 Factorial effect diagram of η

IV. RESULT AND DISCUSSIONS

First, we detected abnormal heart sounds with experimental data and then evaluated the biometrics authentication. The normal heart sounds of ten healthy participants (p1 to p10) were auscultated with a digital stethoscope (Littmann Model 3200) while they were sitting. The sampling rate was 4 kHz, and we measured 30 sec each time. The measurements were repeated 10 to 60 times. The average age of the participants was 22: four men and six women. First, we evaluated the detection performance of the heart murmurs by creating four kinds of unit spaces for each person: p1 to p4. 19 kinds of disease cases (including heart murmurs) were collected from the training workbook's CDs [25, 30]. We precisely classified the heart murmurs based on such generation patterns as systolic heart murmurs, total systolic heart murmurs, and diastolic mid-term murmurs. But in this paper, we collectively refer to them as heart murmurs, which are caused by acute anterior wall infarction and mitral regurgitation, which are also included among heart murmurs. Next, in the personal authentications, we distinguished four people from the other nine.

A. Abnormal heart sound detection

Table II shows the median MD values for the 19 disease cases and healthy participants. The diagnosis described in the training workbook's CD is explained as #1-#14. The personal MD column shows the value for the data of each participant. The first row of p1 is the result calculated with all the features and without data reconstruction. The second row shows the result calculated with all the features after data reconstruction. The third row shows the result calculated with the selected features based on L_{12} after the data reconstruction. The values in the second row are much larger than those in the first row. Therefore, the data reconstruction is effective. The values in the third row are 3 to 7 times larger than those in the second row. Hence, selecting the main features with an orthogonal array is effective for the MD calculations. The procedure in the third row of p1 is applied to the other calculations of p2

to p4. The MD values of the four healthy participants are shown in the Personal MD column: 2.7, 4.1, 1.6, and 1.8.

Next, we investigated the threshold to identify abnormal heart sounds. Fig. 5 shows the relationship between the occurrence rate and the threshold of the MD values. *FRNR* is the false rejection rate of the normal heart sound detections, and *FAAR* is the false acceptance rate of the abnormal heart sounds. We calculated *FRNR* and *FAAR* as follows:

$$FRNR = \frac{\text{false rejected numbers in normal heart sounds}}{\text{all normal heart sound detections}} \quad (4)$$

$$FAAR = \frac{\text{false accepted numbers in abnormal heart sounds}}{\text{all abnormal heart sound detections}} \quad (5)$$

FRNR indicates the occurrence rate at which the MD value of a normal heart sounds exceeds the threshold and shows the error rate that identifies normal heart sounds as abnormal ones. On the other hand, *FAAR* indicates the occurrence rate at which the MD value is smaller than the threshold and shows the error rate that identifies abnormal heart sounds as normal ones.

The MD values and the equivalent error rate (*ERR*) in Table II and Fig.5 are summarized in Table III. The minimum value is 106, which occurs in case 10 in Table II. It is 66 (=106/1.6) times larger than the Personal MD value of p3. When the threshold is a MD value at *ERR*, the recognition rate leads to 100% discrimination of heart murmurs.

Table III
MD and *ERR* for abnormal heart sound cases

ID	MD	Abnormal heart Sounds (19 disease cases)			
		Max. MD	Min. MD	Threshold MD	ERR %
p1	2.7	31231	620	85	5.8
p2	4.1	146103	2427	273	5.2
p3	1.6	5245	106	75	4.9
p4	1.8	16541	329	70	2.1

Table II
Median MD values for abnormal heart sounds and healthy participants

Participant ID	Personal MD	Abnormal heart sound cases including cardiac murmur																		
		1	2	3	4	5	6	7	8	9	10	11	12	13	14	15	16	17	18	19
p1	0.6	6	43	38	41	455	98	81	4	9	8	6	21	23	13	14	16	26	35	47
	2.7	573	4212	3434	3479	8365	4022	2270	185	591	210	532	2043	2431	1064	1079	744	2447	3364	4598
p2	4.1	15403	54190	43922	45183	146103	49443	38352	2427	15395	5598	14325	55944	64692	28569	28981	18942	65160	89909	122337
p3	1.6	332	4887	2045	2051	4552	4459	1259	201	372	106	302	1217	1392	586	604	438	2760	1944	5245
p4	1.8	2007	15428	12893	12936	13012	8115	3645	329	2006	703	1862	7484	8672	3778	3833	2483	8735	12101	16541
Diagnosis		#1	#1	#2	#3	#4	#5	#6	#7	#8	#1	#9	#10	#11	#12	#13	#8	#14	#1	#7

#1: systolic heart murmur, #2: total systolic heart murmur, #3: diastolic middle murmur, #4: diastolic tapering murmur, #5: reflux murmur, #6: acute anterior myocardial infarction, #7: mitral regurgitation, #8: #1 due to aortic valve stenosis, #9 systolic mid-click murmur and contractile late murmur, # 10: early contract murmur, #11: #2 due to tricuspid regurgitation, #12: #2 due to aortic valve stenosis, # 13: #3 due to pulmonary valve stenosis, # 14: S2 overlap due to mitral valve stenosis.

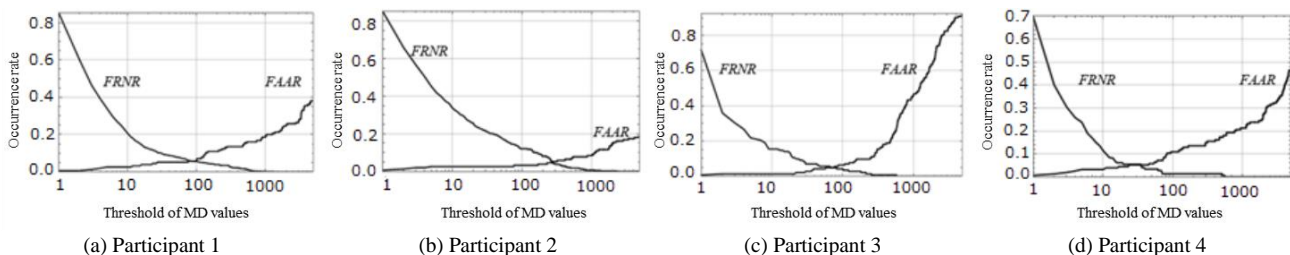


Fig. 5 Relationship between occurrence rate and threshold of MD values

Next, the degree of abnormality is estimated from the change of the MD values shown in Fig. 6 for case 5 in Table II. Features K5 and K6 that refer to heart murmurs are simultaneously and virtually changed against the original values. The vertical axis indicates the MD values, and the horizontal axis indicates the feature times. MD quadratically increases based on the magnification. Therefore, by temporally monitoring the changes of the MD values, abnormal heart sounds will be identified in advance.

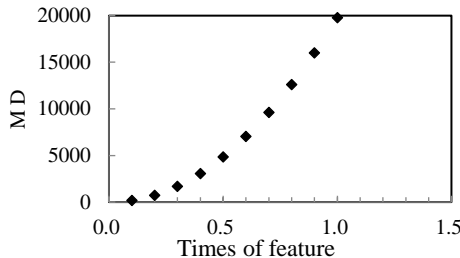


Fig. 6 Example of MD depending on features K5 and K6

B. Personal authentications

We evaluated the performance of the personal authentications. Fig. 7 shows the relationship between the false rejection rate (*FRR*) and the false acceptance rate (*FAR*) of four participants. The MD values were calculated with a round robin of combinations of proposed features. The horizontal axis is the MD threshold, and the vertical axis is the occurrence rate. *FRR* is the proportion of genuine numbers falling below a threshold. *FAR* is the proportion of impostors that exceed it. *FRR* and *FAR* are calculated by the following equation:

$$FRR = \frac{\text{genuine numbers falling below threshold}}{\text{all genuine numbers}} \quad (6)$$

$$FAR = \frac{\text{impostors exceeding threshold}}{\text{all impostors}} \quad (7)$$

Fig. 7(a) shows *FRR* and *FAR* between p1 and the other nine participants. *ERR* is 30% at a MD value of 24. The results in Fig. 7 are summarized in Table IV. The values for each person are underlined: 14, 17, 10, and 16. *ERR* is 16% to 35% for four persons. When the MD values at *ERR* are selected as a threshold, the correct recognition rate (*CRR*) is 90-100%. If the MD value is less than the threshold, the user will be judged as genuine, and the larger one will be judged as an impostor. *CRR* is calculated as follows:

$$CRR = \frac{\text{number of correctly identified subjects}}{\text{all participants}} \quad (8)$$

Table V shows the result calculated with the inverse matrix of Eq. (1). The correct recognition rate is 80-100%. But the MD values are smaller than those calculated by a round robin, and the difference from the threshold is small. This shows that calculating the MD values with a round robin is better.

Previous work used MFCC as a feature for biometric authentications [31-34]. We compared the performance of our proposed features and MFCC by MT. MFCC, which represents a short-period PS of sound waves, is based on human auditory characteristics. In the MFCC algorithm, first, an auscultated heart sound is segmented into a number of cardiac cycles. The PS is computed by a discrete Fourier transform for each frame and summed up on the mel-scale by passing through a mel-scaled triangle filter bank. We obtained eleven kinds of MFCCs by discrete cosine transform. Fig. 8 shows *FRR* and *FAR* calculated with MFCC by a round

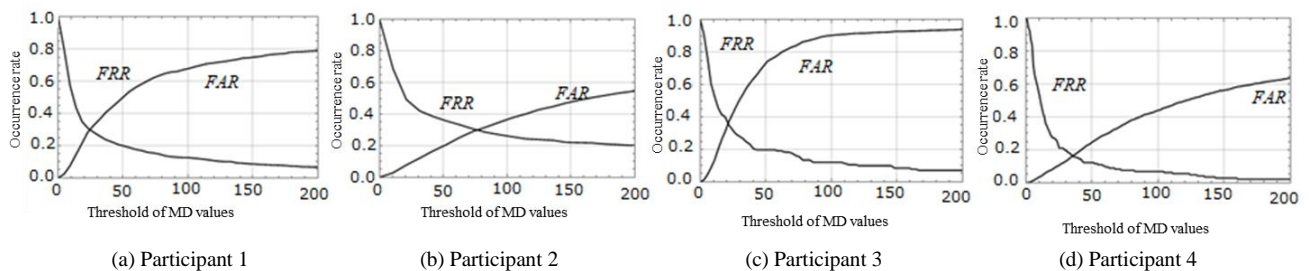


Fig.7 Relationship between *FRR* and *FAR* calculated with proposed features

Table IV
Median MD values and correct recognition rates calculated by round robin

Participant	1	2	3	4	5	6	7	8	9	10	ERR%	Threshold	CRR %
p1	<u>14</u>	36	94	17	124	182	115	333	236	163	30	24	90
p2	109	<u>17</u>	389	40	613	856	682	1726	933	734	30	76	90
p3	16	40	<u>10</u>	33	56	40	41	62	34	41	35	21	90
p4	133	81	628	<u>16</u>	243	971	250	1175	1176	1051	16	35	100

Table V
Median MD values and correct recognition rates calculated by inverse matrix

Participant	1	2	3	4	5	6	7	8	9	10	ERR%	Threshold	CRR %
p1	<u>2</u>	3	9	2	32	19	21	45	21	44	32	3	80
p2	16	<u>3</u>	53	9	303	106	177	411	128	396	29	12	90
p3	2	3	<u>1</u>	2	8	5	6	13	4	10	38	2	80
p4	8	6	29	<u>1</u>	40	49	29	64	49	64	22	4	100

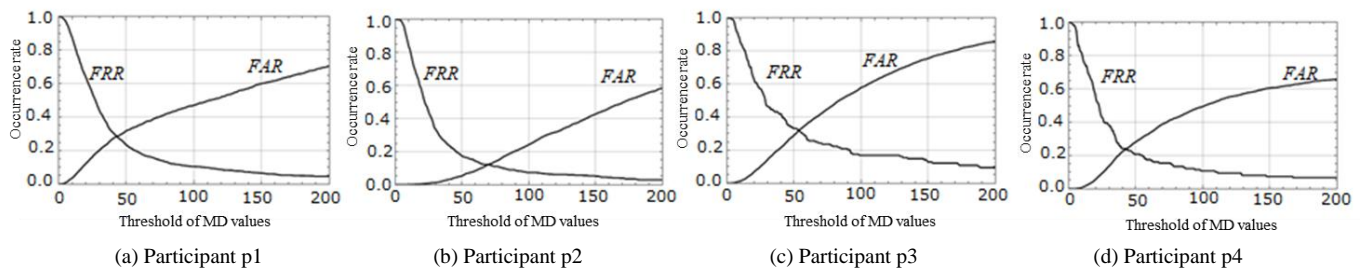


Fig. 8. Relationship between *FRR* and *FAR* calculated with MFCC

Table VI
Median MD values and *CRR* calculated MFCC

Participant	1	2	3	4	5	6	7	8	9	10	ERR%	Threshold	CRR %
p1	28	202	47	26	82	119	145	44	57	65	29	43	90
p2	239	22	133	226	142	129	92	165	180	120	12	69	100
p3	89	128	29	80	57	80	95	70	83	80	32	54	100
p4	59	509	161	24	137	134	284	87	132	104	24	43	100

robin. The calculated results are summarized in Table VI. The *ERR* is 12% to 32%, and the *CRR* is 90-100%. Therefore, our proposed feature produces a similar personal authentication performance.

V. CONCLUSION

We proposed a healthcare authentication system that collects heart sounds as reference data for personal authentication. The MT method detects abnormal heart sounds and achieves personal authentication. We experimentally confirmed the performance of our proposed system, which produced a 90-100% authentication rate for ten research participants and a 100% recognition rate for 19 disease cases of heart murmurs. The heart sounds in this paper were ideal data that reduced noise to clearly auscultate abnormal heart sounds. Therefore, we will verify classification performance with many cases including noise. Future work will verify the biometric authentication performance by increasing the number of samples.

REFERENCES

[1] A. K. Jain, A. Ross, S. Prabhakar, "An introduction to biometric recognition," IEEE Transactions on Circuits and Systems for Video Technology, vol. 14, Issue 1, pp. 4-30, 2004.

[2] Debnath Bhattacharyya, Rahul Ranjan, Farkhod Alisherov A., and Minkyu Choi, "Biometric Authentication: A Review," International Journal of u- and e-Service, Science and Technology, vol. 2, No. 3, pp. 13-26, 2009.

[3] Matsumoto T, Matsumoto H, Yamada K, and Hoshino S, "Impact of artificial gummy fingers on fingerprint systems," International Society for Optics and Photonics, pp. 275-89, 2002.

[4] Erdogmus N and Marcel S., "Spoofing face recognition with 3d masks," IEEE Trans Inf Forensics Secure, 9 (7), pp. 1084-97, 2014.

[5] B. Biggio, Z. Akhtar, G. Fumera, G. L. Marcialis, and F. Roli, "Security evaluation of biometric authentication systems under real spoofing attacks," IET Biometrics, vol. 1, no. 1, pp. 11-24, Mar. 2012.

[6] Akihiro Inomata and Yoshinori Yaginuma, "Hassle-free Sensing Technologies to Monitor Daily Health Changes," FUJITSU Sci. Tech, 50(1), pp. 78-63, 2014.

[7] T. Hashizume and K. Yatani, "Investigating a Photo Plethysmography-enabled Fingerprint Authentication System," IPSJ SIG Technical Report, pp. 1-8, 2017 (in Japanese).

[8] Emna Kalai Zaghouni, Adel Benzina, and Rabah Attia, "ECG based authentication for e-healthcare systems: Towards a secured ECG features transmission," 13th International Wireless Communications and Mobile Computing Conference (IWCMC), 2017.

[9] Emelia J. Benjamin et al., "Heart Disease and Stroke Statistics-2019 Update: A Report From the American Heart Association," Circulation, vol 139, Issue 10, 2019.

[10] Spadaccini A. and Beritelli F., "Human identity verification based on heart sounds," IET Biometrics, vol. 5 (4), pp. 284-296, 2016.

[11] Beritelli F and Serrano S., "Biometric identification based on frequency analysis of cardiac sounds," IEEE Trans Inf Forensics Secure, 2 (3), pp. 596-604, 2007.

[12] Phua K., Chen J., Dat T. H., and Shue L., "Heart sound as a biometric," Journal Pattern Recognition, 41(3), pp. 906-919, 2008.

[13] Foteini Agrafioti and Dimitrios Hatzinakos, "ECG biometric analysis in cardiac irregularity conditions," Springer, SIVIP 3, pp. 329-343, 2009.

[14] M. Abo-Zahhad, Mohammed Farrag, Sherif N. Abbas, and Sabah M. Ahmed: "A comparative approach between cepstral features for human authentication using heart sounds," Signal, Image and Video Processing, 10(5), pp. 843-851, 2016.

[15] Andrea Spadaccini and Francesco Beritelli, "Performance Evaluation of Heart Sounds Biometric Systems on an Open Dataset," 18th International Conference on Digital Signal Processing (DSP), 2013.

[16] Zhidong Zhao, Qinqin Shen, and Fangqin Ren, "Heart Sound Biometric System Based on Marginal Spectrum Analysis," Sensors 2013, 13(2), pp. 2530-2551, 2013.

[17] Zhongwei Jiang and Samjin Choi "Development of Wireless Electronic Stethoscope System and Abnormal Cardiac Sound Analysis Method: Sound Characteristic Waveform Analysis," Transactions of the Japan Society of Mechanical Engineers C, 71(711), pp. 3246-3253, 2005 (in Japanese).

[18] Rashmi C R, Meghashree Y, Meghashree K, Lakshmi Reddy, and Pooja S, "A New Method for Biometric Application Using PCG Signals," International Journal of Emerging Research in Management & Technology, 4(5), pp. 26-31, 2015.

[19] A. Spadaccini and F. Beritelli, "Performance evaluation of heart sounds biometric systems on an open dataset," IEEE 18th International Conference on Digital Signal Processing, 2013.

[20] U. Yadav, S.N. Abbas, and D. Hatzinakos, "Evaluation of PPG Biometrics for Authentication in different states," 11th IAPR, 116(509), pp. 325-332, 2017.

[21] Xinghai Yang, Haili Huang, Jia Ding, Zhen Liu, and Wenjie Fu, "Designing of Heart Sound Diagnostic System Based on OMAP3530," Procedia Environmental Sciences, vol. 8, pp. 307-312, 2011.

[22] Yoshiko Hasegawa, "A Study on Improving Health Examination Diagnosis using Mahalanobis Distance," Japanese Journal of MHTS, vol. 27, Issue 1, pp. 11-23, 2000 (in Japanese).

[23] Hisato Nakajima, Koya Yano, Kei Takada, Ichiro Takagi, Sawako Komiya, Mitsuru Ohata, and Gotaro Toda., "Diseases State Evaluation and Diagnosis by the Change of the Mahalanobis Distance for the Various Types of Liver Diseases," Journal of Quality Engineering Society, vol. 12, Issue 3, pp. 51-58, 2004 (in Japanese).

[24] Nadia Masood Khan, Muhammad Salman Khan, and Gul Muhammad Khan, "Automated Heart Sound Classification from Unsegmented Phonocardiogram Signals Using Time Frequency Features," World Academy of Science, Engineering and Technology International Journal of Computer and Information Engineering, vol.12, no. 8, pp. 598-603, 2018.

- [25] T. Sawayama, "Heart auscultation repeat exercise CD," Japan Medical Publishing, 2015 (in Japanese).
- [26] S. M. Debbal and Fethi Bereksi Reguig, "Frequency analysis of the heartbeat sounds," *Biomedical Soft Computing and Human Sciences*, vol. 13, no. 1, pp. 85-90, 2008.
- [27] V. Nivitha Varghees and K. I. Ramachandran, "A novel heart sound activity detection framework for automated heart sound analysis," *Biomedical Signal Processing and Control* 13, pp. 174-188, 2014.
- [28] Elizabeth A. Cudney, Jungeui Hong, Rajesh Jugulum, Kioumars Paryani, Kenneth M. Ragsdell, and Genichi Taguchi, "An Evaluation of Mahalanobis-Taguchi System and Neural Network for Multivariate Pattern Recognition," *Journal of Industrial and Systems Engineering*, vol. 1, no. 2, pp. 139-150, 2007.
- [29] Takafumi Oohori, Takahiro Yamamoto, Masaki Hori, and Kazuhisa Watanabe, "A Handwritten Chinese Character Recognition by Adaptive Mahalanobis Distance," *IEEE Transactions on Electronics, Information and Systems*, vol. 117, Issue 5, pp. 569-575, 1997 (in Japanese).
- [30] T. Swayama, "Auscultation Training CD," Japan Medical Publishing, 2017 (in Japanese)
- [31] Leigh Anne H Clevenger, "Review of biometric classification of heart sound for continual user authentication and clinical applications," 5th International Conference on Biometrics & Biostatistics, Proceedings of Student-Faculty Research Day, CSIS, Pace University, C1-7, 2016.
- [32] Ferda Dal and I. Yucl Ozbek, "Gender detection with heart sound using MFCC-based statistical features," 10th International Conference on Electrical and Electronics Engineering, 2017.
- [33] A. Spadaccini and F. Beritelli, "Performance evaluation of heart sounds biometric systems on an open dataset," in 2013 18th International Conference on Digital Signal Processing (DSP), pp. 1-5, 2013.
- [34] I. Kamarulafizam, Sh-Hussain. Salleh, J. M. Najeb, A. K. Arif, and A. Chowdhury, "Heart Sound Analysis Using MFCC and Time Frequency Distribution," *World Engineering Congress on Biomedical Engineering and Medical Physics* 2006.

Mizuho Tagashira received a B.S. degree from Tokushima Bunri University, Kagawa, Japan in 2015. She is a clinical engineer and has been with the Brain Attack Center Ota Memorial Hospital, Fukuyama-City, Hiroshima, Japan since 2015. Her research interests include agents of monitoring systems of biological signals in hospitals.

Takafumi Nakagawa received a B.E. degree from Doshisha University, Kyoto, Japan in 1982, a M.S. degree from Miyazaki University, Miyazaki, Japan, in 1984, and a Ph.D. degree from Tokyo University, Tokyo Japan in 2005. He was affiliated with the Mitsubishi Electric Corp. from 1984 to 2014. He is engaged in the electromagnetic analysis of electric devices and particle beam accelerator development. He is currently a professor in the Health and Welfare Department, Tokushima Bunri University. His current research interests include various biometric authentication approaches and data mining.